Environmental Modelling and Software 143 (2021) 105132

Contents lists available at ScienceDirect

Environmental Modelling and Software

journal homepage: www.elsevier.com/locate/envsoft

Forecasting contrasting coastal and estuarine hydrodynamics with OPENCoastS

Anabela Oliveira [a,*], André B. Fortunato [a], Marta Rodrigues [a], Alberto Azevedo [a], João Rogeiro [a], Samuel Bernardo [b], Laura Lavaud [c], Xavier Bertin [c], Alphonse Nahon [a], Gonçalo de Jesus [a], Miguel Rocha [a], Pedro Lopes [a]

[a] National Laboratory for Civil Engineering, Av. do Brasil, 101, 1700-066, Lisbon, Portugal
[b] LIP, Av. Gama Pinto, n.2, piso 3. Complexo Interdisciplinar (3is), 1649-003, Lisboa, Portugal
[c] UMR 7266 LIENSs, CNRS-La Rochelle Université, 2 rue Olympe de Gouges, 17000, La Rochelle, France

A R T I C L E I N F O

Keywords:
SCHISM
Forecast systems
Unstructured grids
Cross-scale
EOSC
Wave and currents modeling
Baroclinic modeling

A B S T R A C T

Robust and accurate coastal forecasts require models to represent the relevant processes, prediction computational tools and reliable computational resources. OPENCoastS is a free, open-source WebGIS platform to develop on-demand hydrodynamic forecast systems that started as a simple 2D engine. OPENCoastS provides a visualization and download interface with in-situ and Sentinel satellite data comparison. 2D tidal, 2D wave & current interaction and 3D baroclinic flows are now included, forced by several atmospheric, oceanic and riverine forcings.

Four applications demonstrate OPENCoastS' capacity. The prediction of the 2020 typhoon season in Taiwan illustrates the use of the service using only large-scale public data. An application to the Bay of Biscay shows the importance of waves on extreme water levels during storms. A nearshore deployment in Figueira da Foz harbor assesses the impact of bathymetry on coupled wave and current circulation. 3D baroclinic circulation forecasts in Tagus estuary are validated by independent data.

1. Introduction

Coastal forecast systems provide predictions of environmental variables at time scales of a few days. Environmental variables include water levels, velocities, wave parameters, pollutant concentrations and sediment fluxes. These forecast systems have a wide range of applications in coastal and harbor management (Viegas et al., 2009; Bedri et al., 2014; Oliveira et al., 2015), civil protection (Breivik and Allen, 2008; Fortunato et al., 2017a; Ferrarin et al., 2019; Stokes et al., 2020), navigation (Orseau et al., 2021), military operations and recreation (e.g. windguru.cz, magicseaweed.com). Some of these forecast systems cover spatial scales from oceans and regional seas to coastal regions, using downscaling techniques over structured and unstructured grids (Trotta et al., 2016, 2021). They are developed and operated by research centers, meteorological and hydrographic organizations, harbor administrations and private companies.

In spite of the growing development of coastal forecast systems, their dissemination remains limited by their implementation and maintenance costs. These costs are mostly associated with very specialized human resources, with backgrounds in both numerical modeling and information technologies, and also with dedicated computational resources to guarantee a timely delivery of predictions.

However, several evolutions are paving the way for a drastic increase in the development and adoption of coastal forecast systems. First, higher resolutions, more stable numerical schemes and better parameterizations reduce the need for calibration and the effort required to optimize the numerical parameters. As a result, the skills required from modelers decrease and forecasts become more robust. Second, the growing availability of online near-real time data (e.g., GEBCO, EMODNET), atmospheric forecasts (e.g., GFS, WRF, ARPEGE) and large-scale ocean models (e.g., FES2014, CMEMS, HYCOM) provide free access to the information required to force local forecasts worldwide. Third, large computational infrastructures, both public and commercial, can now provide the computational power to perform demanding simulations without the need to acquire and operate these infrastructures. The European Open Science Cloud (EOSC) and the Partnership for

* Corresponding author.
E-mail address: aoliveira@lnec.pt (A. Oliveira).

https://doi.org/10.1016/j.envsoft.2021.105132
Accepted 9 July 2021
Available online 13 July 2021

Advanced Computing in Europe (PRACE) are examples of such public infrastructures.

A fourth evolution that can drastically reduce the cost of generating and operating coastal forecast systems is automation. The recent development of Web-based platforms that can simultaneously generate and operate coastal modeling systems with minimal human intervention will reduce the cost of forecast systems, thereby fostering their dissemination. Examples of these tools remain scarce in the coastal and ocean communities. WebMARVL (the Virtual Marine Laboratory, Oke et al., 2016), for setting up ocean circulation and wave models, Delft-FEWS, dedicated to hydrological and coastal flood forecasting (Werner et al., 2013), and OPENCoastS, to generate coastal forecast systems for any location in a few minutes (Oliveira et al., 2020) are the most comprehensive platforms available. OPENCoastS is a user-friendly platform supported by EOSC computational services and resources. It is freely available to all users whereas, for instance, WebMARVL is dedicated to the Australian communities. The original version of the platform described in Oliveira et al. (2020) was however limited to simple physics (i.e., 2D depth-averaged shallow water flows). Now it has matured and addresses more complex flows, including wave and currents interactions and 3D baroclinic flows. The only inputs requested to the users to set up a new deployment are the horizontal grid file and, for the 3D runs, also the vertical grid. The platform is maintained in operation through the use of European Open Science cloud (EOSC) resources and forecasts still take only a few minutes to generate.

This paper aims at demonstrating how forecast systems built using the OPENCoastS service can provide accurate prediction of complex flows in estuarine and coastal environments. “Complex flows” refer here to flows associated with extreme atmospheric events, breaking waves, and strong density gradients, and at scales ranging from tens of meters to thousands of kilometers. Four demonstration examples are presented herein that cover various spatial scales (from basin-wide to estuarine scales), different forcing agents (tides, waves, river flow, wind and atmospheric pressure), applied in distinct geographies (European and Asian coasts). These examples address different scientific questions (e.g., coastal inundation, salinity dynamics in estuaries) and the forcing agents include tides, waves, river flow, wind and atmospheric pressure. The criteria behind the selection of the applications are summarized in Table 1. The evolution of the platform, from its original version to its present capabilities, is also detailed to promote the usage of the service software by other teams. It is now freely available under licence Apache License Version 2.0 at https://gitlab.com/opencoasts/eosc-hub/webportal.

The paper is organized as follows. First, the OPENCoastS platform is briefly described, with an emphasis on the most recent features. Then, the capabilities of the platform to support operational management in coastal systems are demonstrated through four examples of application. In section 3, these examples are used to illustrate and discuss the lessons learned from the first three years of development of OPENCoastS. Finally, the potential and the present limitations of OPENCoastS are discussed and its evolution is anticipated.

Table 1
Characterization of the demonstration cases.

	Coast of Taiwan	Bay of Biscay	Figueira da Foz Harbor	Tagus Estuary
basin scale	X	X		
coastal/ estuarine scale			X	X
2D barotropic	X	X	X	
3D baroclinic				X
waves		X	X	
no waves	X			X

2. OPENCoastS service version 2: general description

2.1. Overview of the OPENCoastS service

The OPENCoastS service provides accurate circulation forecasts in any coastal system of choice (Oliveira et al., 2020). This is achieved through the use of the process-comprehensive suite of numerical models provided by SCHISM (Zhang et al., 2016), and of a complex computational web platform. SCHISM was chosen because it encompasses all relevant processes, and the web platform was built to run it seamlessly and automates the whole prediction workflow. This combination provides the users the capacity to efficiently build, manage and visualize forecasts. Initially developed as a simple 2D forecast engine (Oliveira et al., 2020), OPENCoastS is now a full-fledged service that simulates all types of estuarine and coastal circulation options: 2D barotropic, 2D waves and currents interaction and 3D baroclinic circulation. Herein, we start by summarizing the architecture and main characteristics of the service and its implementation in the EOSC infrastructure. The implementation of the new circulation functionalities and their dependencies for input file building is detailed afterwards, along with the new options for both ocean forcings and data comparison.

The OPENCoastS service aims at addressing the following properties: Broad availability, Simplicity and user-friendliness, Comprehensiveness, Accuracy and reliability, Flexibility and Modularity (Oliveira et al., 2020). These properties are achieved in the current full circulation service, to guarantee the quality of the final forecasts. Moreover, the architecture to address the properties of modularity and flexibility is paramount to continue to accommodate any new functionalities in the future while maintaining a coherent, simple and user-friendly platform. The service is available at https://opencoasts.ncg.ingrid.pt and is organized along the “Configuration assistant”, which guides the assemblage of the site-specific forecast systems; the “Forecast systems manager”, through which users monitor and act upon their forecasts; and the “Outputs viewer” where users visualize and download model’s input and output files (Fig. 1). The complete workflow of the Configuration assistant in the OPENCoastS web app is summarized in Fig. 2, highlighting the detailed approach to account for the several circulation options requirements.

2.2. Current application of SCHISM modeling suite in OPENCoastS

The OPENCoastS evolution to complete coastal physics was made possible by the comprehensive representation of physical processes available in the SCHISM modeling suite (Zhang et al., 2016; http://ccrm.vims.edu/schismweb), the open-source modeling engine behind OPENCoastS. SCHISM is an open-source community-supported modeling system designed for a seamless cross-scale simulation from creek to ocean and is used here in version v5.4.1. The model is fully parallelized, to optimize the computing times in forecast applications.

SCHISM has been extensively tested against ocean/coastal benchmarks (Chen et al., 2013; Lynett et al., 2017) and applied to several regional seas, embayments and estuaries worldwide in the fields of general circulation, tsunami, storm-surge and compound inundation, wave-current interaction, water quality, coastal ecology, and morphodynamics (e.g., Guérin et al., 2016; Rodrigues and Fortunato, 2017; Fortunato et al., 2017b; Allen et al., 2018; Li et al., 2018; Du et al., 2020; Wang et al., 2020; Lavaud et al., 2020; Huang et al., 2021). SCHISM is also the hydrodynamic engine of several forecast systems besides OPENCoastS (Stanev et al., 2016; Fortunato et al., 2017a; Chiu et al., 2018; Fernandez-Montblanc et al., 2019).

SCHISM solves the three-dimensional shallow water equations and computes the free-surface elevation and the 3D water velocity, salinity and temperature fields using finite-element and finite-volume schemes. The simultaneous solution of continuity and momentum equations, and a highly efficient semi-implicit finite-element Eulerian-Lagrangian algorithm bypass the most severe stability restrictions (e.g. associated

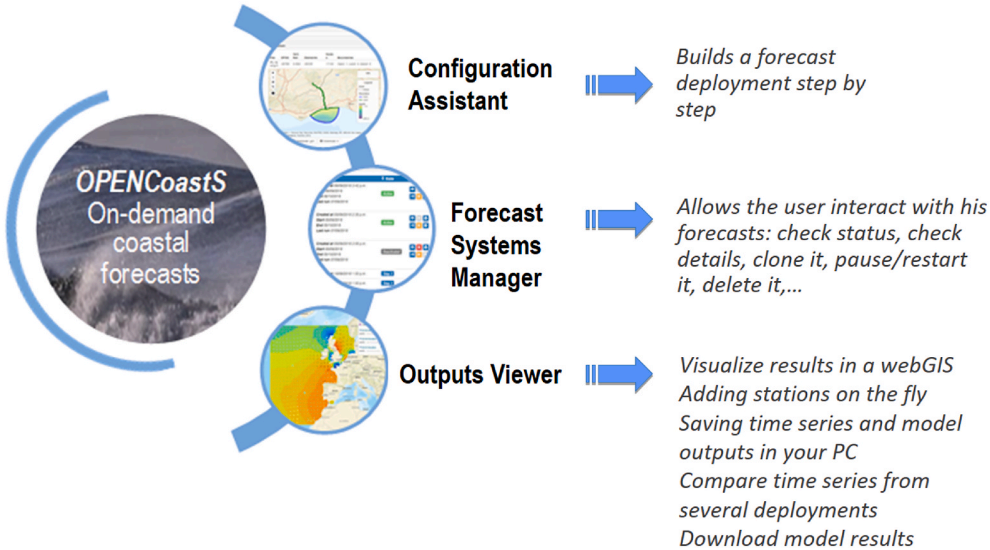

Fig. 1. OPENCoastS frontend components.

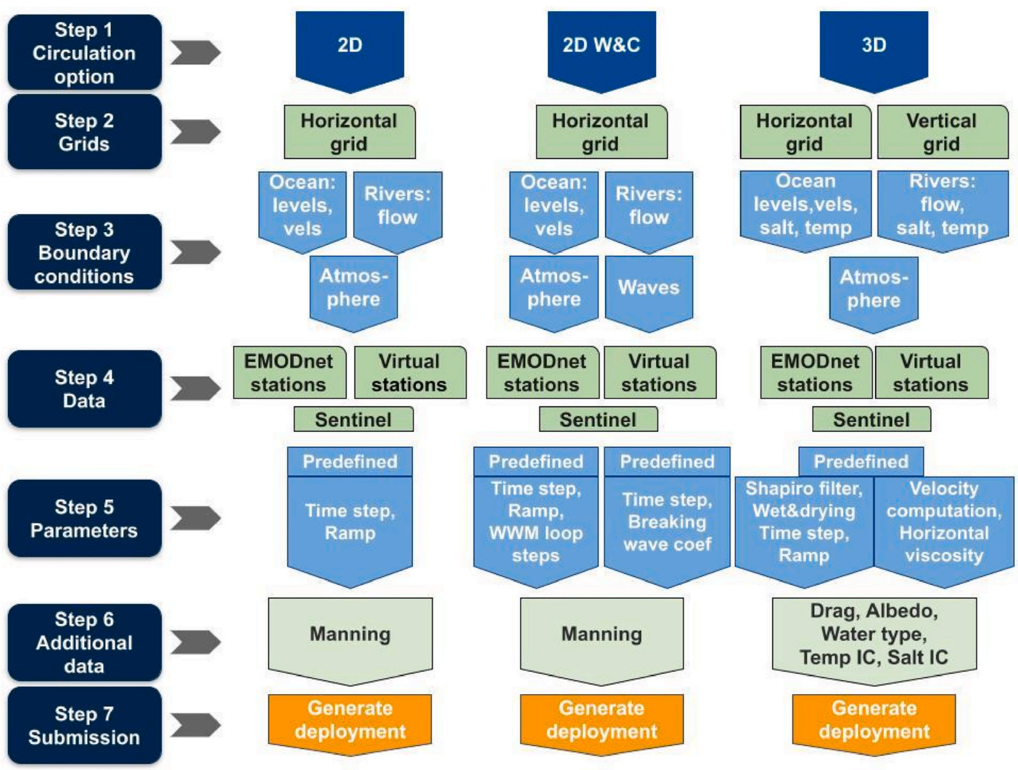

Fig. 2. Workflow of the Configuration assistant for the several circulation options.

with the Courant number). Mass conservation can be enforced by upwind or finite-volume transport algorithm (TVD2) methods. The natural incorporation of wetting and drying makes the model suitable for inundation studies. In OPENCoastS, the wave model WWM (Roland et al., 2012) is fully coupled in 2DH with SCHISM, and the two models share the same computational grid and domain decomposition. When this option is activated, WWM provides the circulation model with wave forces computed according to the radiation stress formalism of Longuet-Higgins and Stewart (1964) and the circulation model provides WWM with fields of water levels and depth-averaged velocities. SCHISM discretizes the domain using unstructured grids in the horizontal, which allows a greater flexibility in representing the bathymetry, and hybrid SZ coordinates or LSC[2] (Zhang et al., 2015) along the vertical.

In OPENCoastS, only horizontal grids with triangular elements and vertical grids based on hybrid SZ coordinates can be used, in spite of other discretization options available in SCHISM. Forcing conditions at the ocean boundaries in OPENCoastS include both elevation and velocities if FES2014 is used, providing more accurate results, or just elevations, for the other forcing options. For 3D simulations, forcing conditions at the oceanic boundaries also include space and time varying salinity and temperature. At the river boundaries, forcing conditions can be set up as constant or as time varying. Those include river flows for 2D simulations and river flows, salinity and temperature for 3D simulations. OPENCoastS is organized along three circulation options, depending on the relevant physics. A summary of the inputs and outputs is presented below along with the new features.

1) 2D barotropic simulations

These simulations output water levels and depth-averaged velocities. The circulation is forced by tides, wind, atmospheric pressure and river flow. This option corresponds to the first version of OPENCoastS, with a minor improvement of forcing both elevation and velocities at the ocean boundaries. The reader is referred to Oliveira et al. (2020) for further details.

2) 2D barotropic simulations with wave-current interaction (2D W&C)

In addition to Option 1, these simulations also provide wave parameters. All wave-current interactions are simulated, including the effect of water levels and depth-averaged currents on wave propagation and the wave forces on the mean flow through the wave radiation stress gradients. Inside the domain, WWM is forced by the same surface winds as the circulation model. WWM is also forced along its open boundaries by time series of directional spectra computed from an application of the WaveWatch III model (WW3, version 5.16) (The WAVEWATCH III R Development Group, 2016) to the North Atlantic (grid is shown in Supplementary material #1). As spectra for larger domains are not freely available online, this option can only be used for domains forced by North Atlantic waves. Each deployment has its own WW3 runs, to generate the necessary boundary conditions. A master WW3 is also maintained to provide hot-start conditions for each new deployment's forcing WW3 run (Fig. 3), avoiding cold-start conditions or the need to start the forecast deployment several days in the past. The wave and current backend workflow is highlighted in Fig. 3.

3) 3D baroclinic simulations - these simulations provide 3D fields of velocity, salinity and water temperature, besides water levels. They can be forced by tides, river flow, temperature and salinity at all the boundaries, and also by the atmospheric surface forcing (wind, air temperature, pressure, humidity, solar radiation and downwelling longwave radiation).

Boundary conditions for 3D velocities, salinity and temperature at the ocean boundaries are provided by CMEMS (https://marine.copernicus.eu/), with two sources available: CMEMS Global and Iberian-Biscay-Ireland (IBI) regional seas. These sources can also be used to force water elevations in other circulation options as part of the ocean boundary conditions portfolio. Atmospheric inputs for these runs can be obtained with GFS or WRF, both provided by NOAA. At the rivers' boundaries, besides annual and monthly values, a web provider for time series can also be used to provide flow forecasts every day. Finally, one river flow can also be specified as a percentage of another one, either defined as monthly or annual values or through an external river forecast provider.

Unlike the wave and current interaction option, 3D baroclinic forecasts can be generated anywhere in the world. The forcing of the salinity and temperature ocean boundaries can only be done with one of the two CMEMS options: Global or IBI.

The Forecast systems manager provides multiple actions on forecasts 1) conclude deployment; 2) pause and cancel a deployment and 3) cloning a deployment, besides monitoring the status of the runs and providing alerts for the near conclusion of the operating period. The cloning facility is used frequently as it provides a very efficient way to perform sensitivity analyses on parameters and forcings for a specific site.

The Outputs viewer presents results from all circulation options. Besides the inclusion of the new variables depending on the type of deployment selected, the capacity to see 3D results along the vertical (and to compare different levels) was also added. Downloading facilities were extended for the new files generated in the additional options.

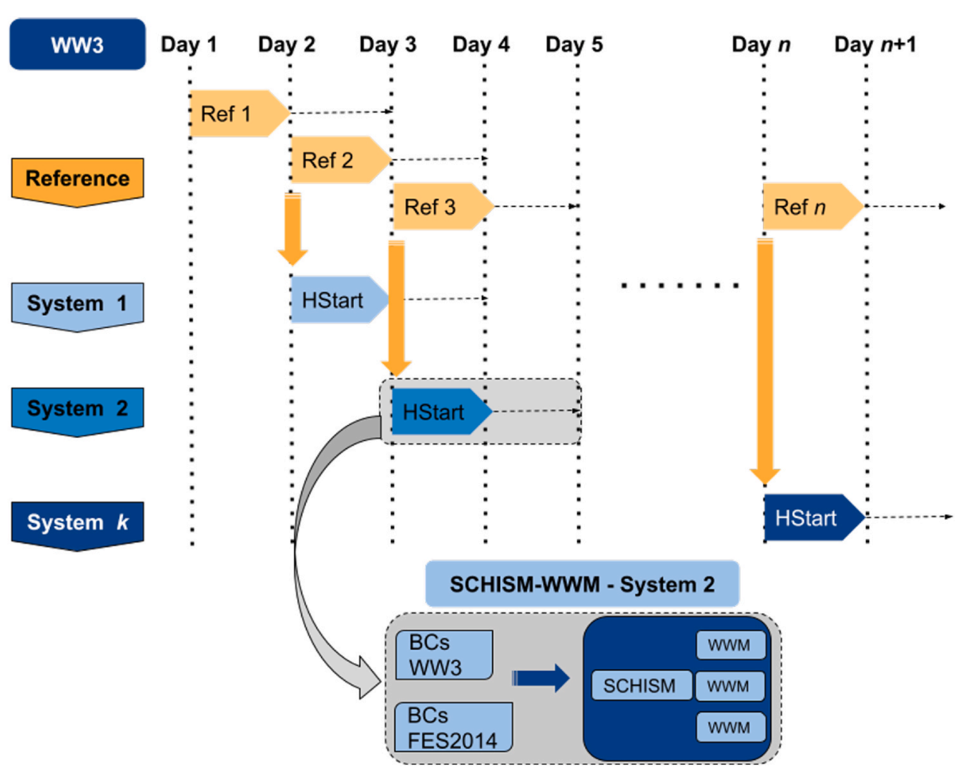

Fig. 3. Backend workflow for waves & currents option: procedure for hot starting the waves' simulation. The inset illustrates the procedure for each simulation, with the possibility of having multiple WWM runs for one time step of SCHISM or the opposite situation.

2.3. Data comparison options in OPENCoastS

Automatic comparison with field data validates the quality of the predictions and supports the usefulness of the tool and the users' confidence in its results. OPENCoastS is linked to the EMODNET Physics elevation data hub (https://portal.emodnet-physics.eu/). The user selects the stations for the model/data comparison for each deployment in the Configuration assistant and then visualizes the data against the results in the viewer.

Comparison with remote sensing data is also available, to determine the interface between land and water (extent of inundation), based on images from the Sentinel satellites. The possibility of comparing model results with a processed Sentinel image is integrated in the Configuration assistant. If the user selects the comparison with remote sensing option, the OPENCoastS workflow starts a regular procedure to download images from the ESA Copernicus OpenHub, crops them to the limits of the deployment horizontal grid, binarizes it to determine the land-water interface and converts it to a raster. The rasters are stored in a database and are connected to the respective deployment ID. Upon entering the viewer page, the OPENCoastS interface builds a JSON file with the latest rasters.

In the viewer, the users can select the visualization of the Sentinel-based layers against the model results. As Sentinel images have a specific time stamp, we provide the capacity to overlap each simulation with the nearest processed image. This visual comparison is available for the whole simulation, regardless of the specific time step that would be closest to the Sentinel time stamp. The rasters are loaded into the map with an opacity applied to them to facilitate the comparison with the model forecasts (Fig. 4).

New satellite images are downloaded and added to the system at the beginning of each day. Upon selecting the option to download the images, as there will not be any images available on the database, OPENCoastS checks back in time to retrieve the images available from the last five days.

2.4. Brief description of the implementation of OPENCoastS in the EOSC infrastructure

During the last decade, Global Open Science emerged as a trusted digital platform to support the scientific community. The European project EOSC-hub aimed to foster the best practices for data and services management, simplifying the researchers' access to available infrastructure sites. OPENCoastS is one of the seven thematic services integrated in the EOSC infrastructure in the scope of this project (https://marketplace.eosc-portal.eu/services/opencoasts-portal).

The OPENCoastS service requires high availability of computational resources to guarantee the delivery of forecast outputs in due time. Portugal's National Distributed Computing Infrastructure (INCD) and Cantabria Physics Institution (IFCA) offer the required facilities for OPENCoastS simulations, providing the integration with the core EOSC-hub services for authentication, accounting, computation and data preservation.

OPENCoastS comprehends several components, such as catalogs of model data/results and their metadata, SCHISM processing scripts, a web Configuration assistant, a web portal for managing the user accounts and applications, and a web map visualization tool. These components were integrated with the EOSC core services summarized in Fig. 5. Available core services were promoted within EOSC-hub to support OPENCoastS and other thematic services (https://marketplace.eosc-portal.eu/services/c/access-physical-einfrastructures).

The main supporters of those core services are the European Grid Initiative (EGI), for cloud and grid services, and EUDAT for storage. Authentication Authorization and Identity (AAI) is available in both EUDAT and EGI portfolios, which implement the AARC Blueprint Architecture (https://aarc-project.eu/architecture/), supporting communities users' with subordinate end services.

The current implementation of OPENCoastS in the INCD infrastructure uses the following core services: EGI Cloud Compute, EGI Online Storage and EGI Check-in for AAI. These EOSC core services enable the deployment of the OPENCoastS applications and provide the endpoint for the portal. Additionally, SCHISM's processing work and all related tasks are submitted to EGI Workload Manager. This manager distributes the computational demand by all available resource sites using EGI High-Throughput Compute. The software requirements and dependencies are encapsulated in a docker image that is loaded in the computing nodes with the udocker tool (Gomes et al., 2018). Udocker allows pulling and executing docker containers in Linux batch systems and interactive clusters in user space without requiring root privileges. A bundle that encapsulates the whole OPENCoastS service and its installation at a user-defined infrastructure is freely distributed at the GitLab repository in https://gitlab.com/opencoasts/eosc-hub/webportal.

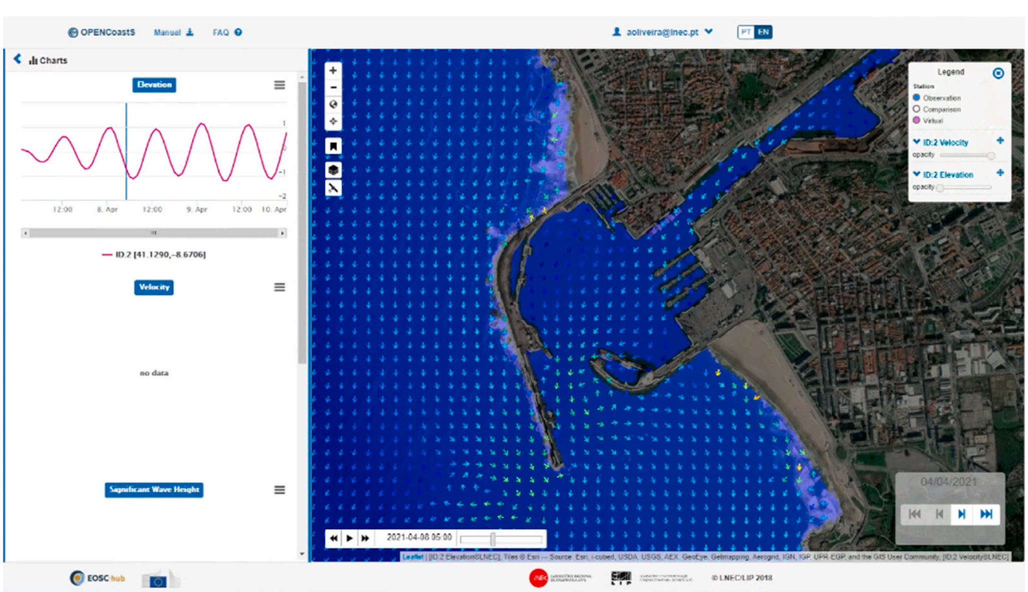

Fig. 4. Comparison between the water limit extracted from Sentinel 2 images (in blue) and the OPENCoastS prediction (velocity field). The brown dashed line marks the limit of the grid, which represents the Leixões harbor and Matosinhos Beach in Northern Portugal.

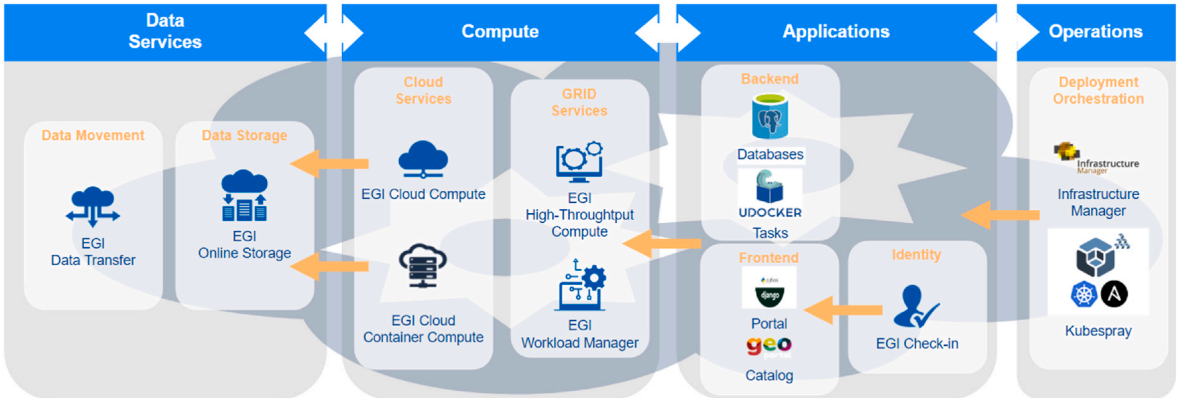

Fig. 5. OPENCoastS integration with EOSC services.

3. OPENCoastS applications

3.1. Extreme water levels in the coast of Taiwan

The northwestern Pacific Ocean is the most active tropical cyclone basin on Earth (Elsner and Liu, 2003). The most severe of these cyclones, locally known as typhoons, can generate extreme storm surges that can have devastating effects on the shores of the Philippines, China, Taiwan and Japan. Here, we illustrate the generation of a forecast system for the coast of Taiwan with OPENCoastS and its validation using only publicly available data.

Typhoon tracks can be divided into three groups (Elsner and Liu, 2003). Taiwan is affected by typhoons following two of these groups: the straight track, a general westward path, and the parabolic recurving track, which follows to the North-west and then turns north. The model domain (Fig. 6) was thus defined such that it contains these typhoon tracks. The coastal boundary was defined using the Global Self-consistent, Hierarchical, High-resolution Shoreline database (https://gnome.orr.noaa.gov/goods/tools/GSHHS/coast_subset), and the bathymetry was extracted from the General Bathymetric Chart of the Oceans (https://download.gebco.net). A grid with 93,000 nodes was generated by automatically placing the nodes with a specified spatially-varying resolution using the program xmgredit (Turner and Baptista, 1993). This resolution varies between 1 and 2 km around Taiwan and 10–16 km in the deep ocean. Then, this preliminary grid was automatically improved using the program nicegrid (Fortunato et al., 2011). The resulting number of elements linked to each node varies between 5 and 7 to ensure a smooth transition between element sizes. Because the domain is very deep, friction is expected to be negligible. The Manning coefficient was set to 0.022 $m^{1/3}/s$ throughout the domain, and the model was not calibrated. The time step was specified as 240 s, as proposed by OPENCoastS.

SCHISM was forced at the sea surface by winds and atmospheric pressure from GFS, and at the open boundaries by tides from FES2014

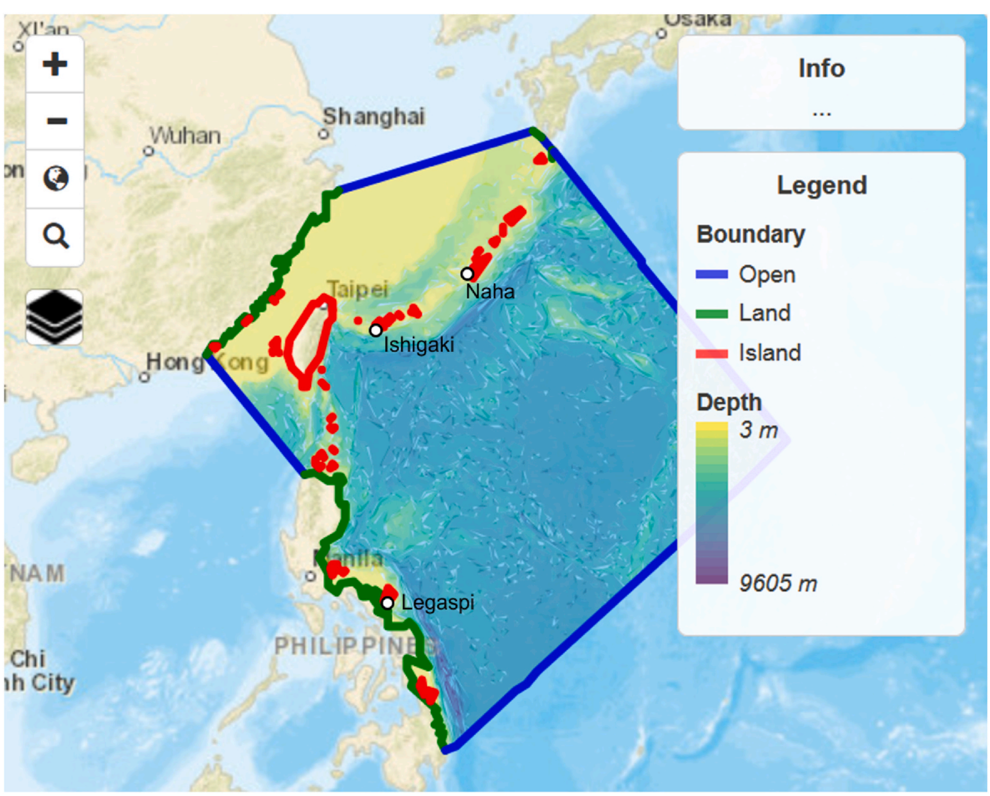

Fig. 6. Taiwan typhoon model domain, bathymetry and tide gauges (circles).

(Lyard et al., 2020) and the inverse barometer effect.

Forecasts were produced in OPENCoastS for the 2020 typhoon season (July to September). During this period, 14 tropical storms occurred in the Pacific, including typhoons Hagupit (July 31 – August 5), Bavi (August 21 – August 27), Maysak (August 27 – September 3) and Haishen (August 31 – September 9). Haisen, in particular, peaked as a Category 4 typhoon. The model was validated using sea surface height data from the three stations located within the domain (Fig. 6) and available at the EMODnet platform. The data time series include numerous gaps.

Comparison with field data shows that the model reproduces sea surface heights with unbiased root mean square errors between 5 and 10 cm (Table 2). These errors correspond to 12–25% of the standard deviation of the measured sea surface height. The RMSE obtained with OPENCoastS compare favorably with a recent application to the same area (Liu and Huang, 2020).

The model accuracy could certainly be improved. A comparison between the shoreline database and satellite images shows that the data are coarse and outdated in some areas. Calibration of the friction coefficient in the continental shelf between Taiwan and China, which would require tide gauge data in that area, would probably improve the water levels prediction locally. More importantly, including waves would increase the storm surge. The importance of waves on storm surges was shown by Chen et al. (2017) for this particular region, and is also shown in the next section for the Bay of Biscay.

In spite of these limitations, this application shows that adequate forecasts can be quickly obtained with OPENCoastS without any a priori knowledge of the study region and using only open data and model results for the model setup and validation.

3.2. Storm waves and surge in the Bay of Biscay

The Bay of Biscay is exposed to severe winter storms, which can drive waves of significant height (hereafter Hs) over 10 m, storm surges over 1.5 m (Bertin et al., 2015; Lavaud et al., 2020) and catastrophic marine flooding (Bertin et al., 2014). The storm Justine hit the central part of the Bay of Biscay on 31st of January 2021 and drove waves of Hs reaching 10 m in the deep ocean and over 8 m at the nearshore buoy Cap Ferret (Fig. 7). Inside the Arcachon Lagoon (Fig. 8), water level measurements suggest that a storm surge of about 1.0 m developed. In this section, we present a fully-coupled 2DH high resolution forecast of the sea state and water levels associated with this storm to demonstrate the relevance of short waves in OPENCoastS.

The unstructured grid used to perform the forecast covers the southern part of the Bay of Biscay (Fig. 7) and comprises 60060 nodes and 117303 triangular elements, with a spatial resolution ranging from 5500 m along the open boundary to 80 m at the entrance of the Arcachon Lagoon. Along the open boundary, the circulation model was forced by amplitudes and phases of the 34 main tidal constituents from FES2014 (Lyard et al., 2020). Over the whole domain, the circulation model was forced by 10 m wind speed and sea-level pressure issued from ARPEGE atmospheric forecasts and an inverse barometer condition was applied along the open boundary. ARPEGE wind fields were also used to force the wave model WWM. Along the open boundary, WWM was forced by time-series of directional wave spectra, which were computed from WW3 forced with wind fields from the GFS atmospheric model. The time steps were set to 30 s and 300 s in the hydrodynamic and wave model, respectively.

Table 2
Validation of the Taiwan forecasts: unbiased root mean square errors (URMSE) and normalized unbiased root mean square errors (NURMSE). NURMSE are normalized by the standard deviation of the data.

Station	Ishigaka	Legaspi	Naha
URMS (m)	0.10	0.05	0.07
NURMS (%)	25	12	14

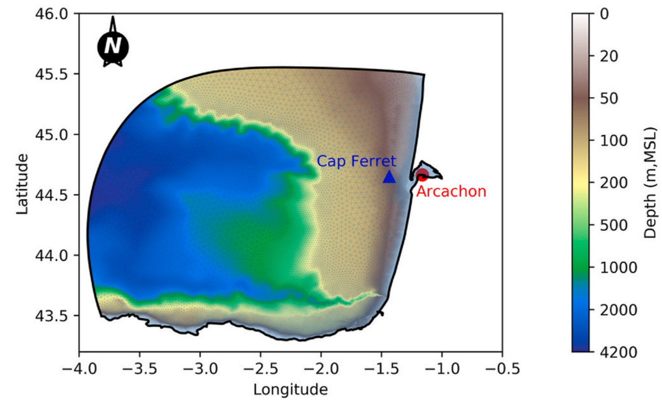

Fig. 7. Bathymetric map and extension of the computational domain with location of the Arcachon tide gauge (red circle) and the Cap Ferret buoy (blue triangle).

The model predictions were first compared against observed significant wave height (Hs), mean absolute wave period (Tm02) and mean wave direction (Mwd) available at the Cap Ferret Buoy, located 14 km from the coast by a mean water depth of 50 m. This comparison reveals that Hs and Tm02 are very well reproduced, with normalized root mean square errors (NRMSE) of 12 and 8%, respectively. Mwd is also well reproduced, with a root mean square error (RMSE) lower than 5° (Fig. 8).

Water levels were measured inside the Arcachon Lagoon (Fig. 9) and the storm surge was computed as the difference between the observations and a tidal prediction based on a harmonic analysis performed over a 5-year time series using U-Tide (Codiga, 2011). For the model, the storm surge was computed as the difference between simulations including tides and surge and a simulation that is forced only by tides. The comparison between observed and modeled storm surges reveals firstly that without wave forces, the model underestimates the surge peak by a factor of 3. When short waves are included in the simulation, this strong negative bias is cancelled out and the RMSE is reduced by a factor of 3 (Fig. 9). For the total water level, including short waves also removes a 0.27 m negative bias and reduces the RMSE by a factor of 3. This behavior was already observed by Lavaud et al. (2020), for the storm Klaus (2009), and explained by the dissipation of storm waves at the entrance of the Arcachon Lagoon, which drives a large wave setup that extends at the scale of the whole lagoon. This new application demonstrates that the results of Lavaud et al. (2020) were not specific to a particular storm and suggest that short waves should be included in storm surge forecasts when intense wave breaking occurs at the entrance of estuaries and lagoons.

3.3. Impacts of bathymetric changes on forecasted nearshore circulation at Figueira da Foz

3.3.1. Motivation and goals

In nearshore areas, short-term predictions of coastal hydrodynamics are useful for harbor navigation, bathing safety and civil protection. Because these areas are shallow, the hydrodynamic conditions can be affected by bathymetric changes. These changes can occur rapidly due to both natural and anthropogenic causes, such as storm-driven erosion or dredging and deposition. Thus, the accuracy of model predictions could depend on frequent updates of the bathymetry.

To assess this dependence, sensitivity tests to observed bathymetric evolutions were performed near a jettied tidal inlet on the western coast of Portugal. These tests were made using an OPENCoastS forecast, and illustrate how the platform can be exploited for hindcast runs. Indeed, these hindcast runs were done using the input files created and made available through the forecast runs. The forecast was initially

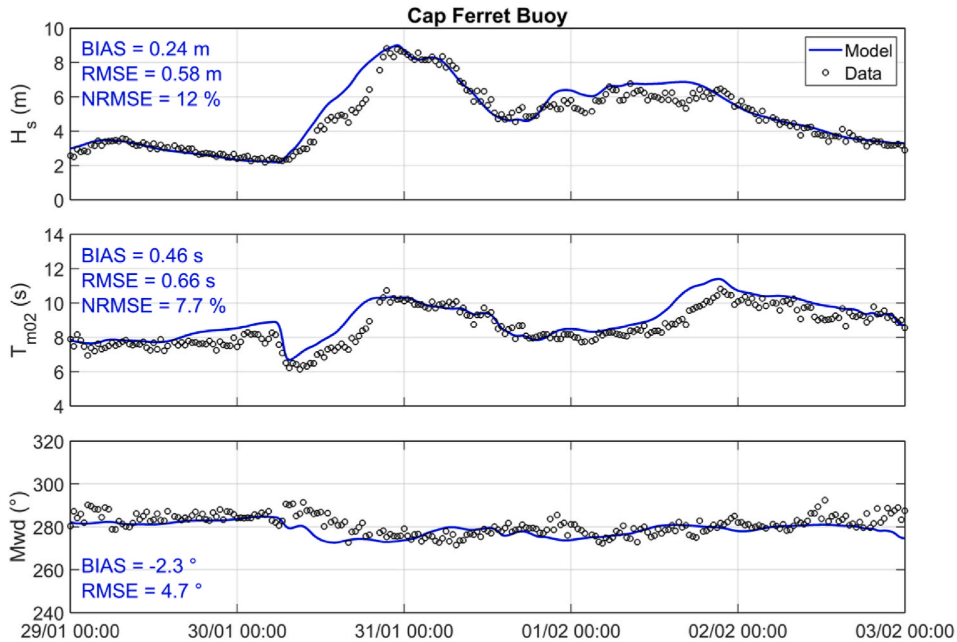

Fig. 8. Modeled (blue) against observed (black circles) significant wave height (Hs), mean absolute wave period (Tm02) and mean wave direction (Mwd) at Cap Ferret Buoy during storm Justine. Normalized root mean square errors (NRMSE) are normalized by the mean of the data.

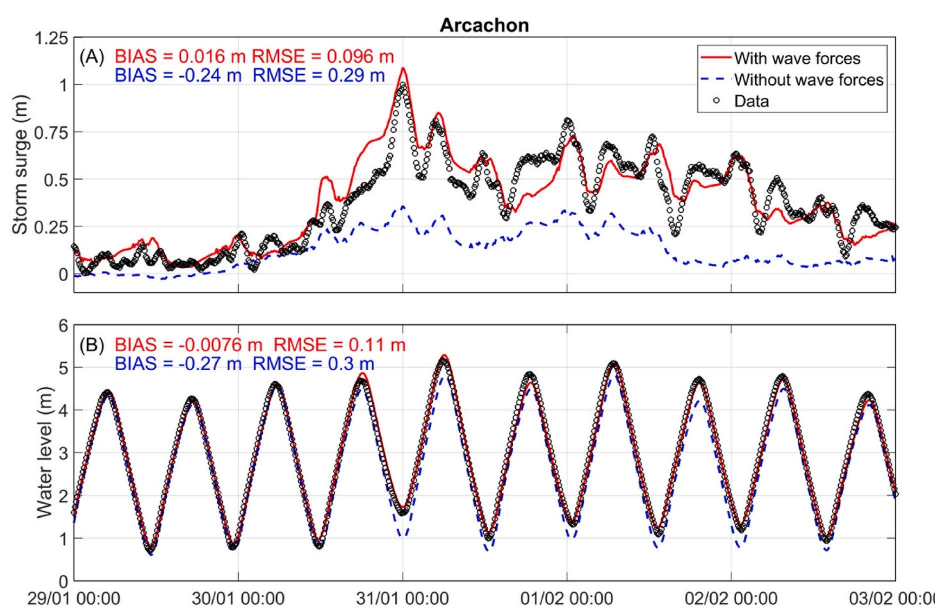

Fig. 9. (A) Observed (black circles) against modeled storm surge with (blue) and without (red) short waves and (B) same for total water levels.

implemented for the nearshore area in the vicinity of the harbor of Figueira da Foz (Fig. 10a), following the 2D W&C workflow (Fig. 2). The unstructured grid has about 50,000 nodes and extends from 84 m water depth offshore to 14 km upstream the Mondego estuary; the grid spatial resolution ranged from 2.5 km offshore to 20 m in the nearshore area and along stream, and the timestep was set to 30 s. The forecast system (Nahon et al., 2020) was implemented in OPENCoastS with a bathymetry surveyed in the summer 2019 (ebb-tidal delta and subtibal sandbars) and March 2020 (intertidal beach). The model skill is evaluated for offshore and nearshore significant wave height, and nearshore, harbor and river water level elevation and is summarized in Table 3.

3.3.2. Measured bathymetric changes

The sensitivity of the model results to the bathymetry was assessed considering two bathymetries in addition to the one from 2019/20 used in the forecast system. The first bathymetry was used to investigate the consequence of the inflow of sediments from the beach and sandbars to the north of the inlet's northern jetty. During storms, this inflow of sediments can rapidly accrete the access channel (S1 location, Fig. 10b), as, for example, during the storm Epsilon in October 2020 (Fig. 11b). A post-Epsilon survey, made on 6 November 2020, was then used to modify the reference bathymetry and assess the impacts on waves and current predictions.

In recent years, the sand brought in by (storm) waves is dredged and deposited in front of Cova Gala Beach, to the south of the inlet's southern jetty. In 2018, these deposits created a protuberance of the ebb-tidal delta. Initially within 6 m–10 m depth (chart datum), the deposit subsequently spread and evolved into large nearshore sandbars visible in

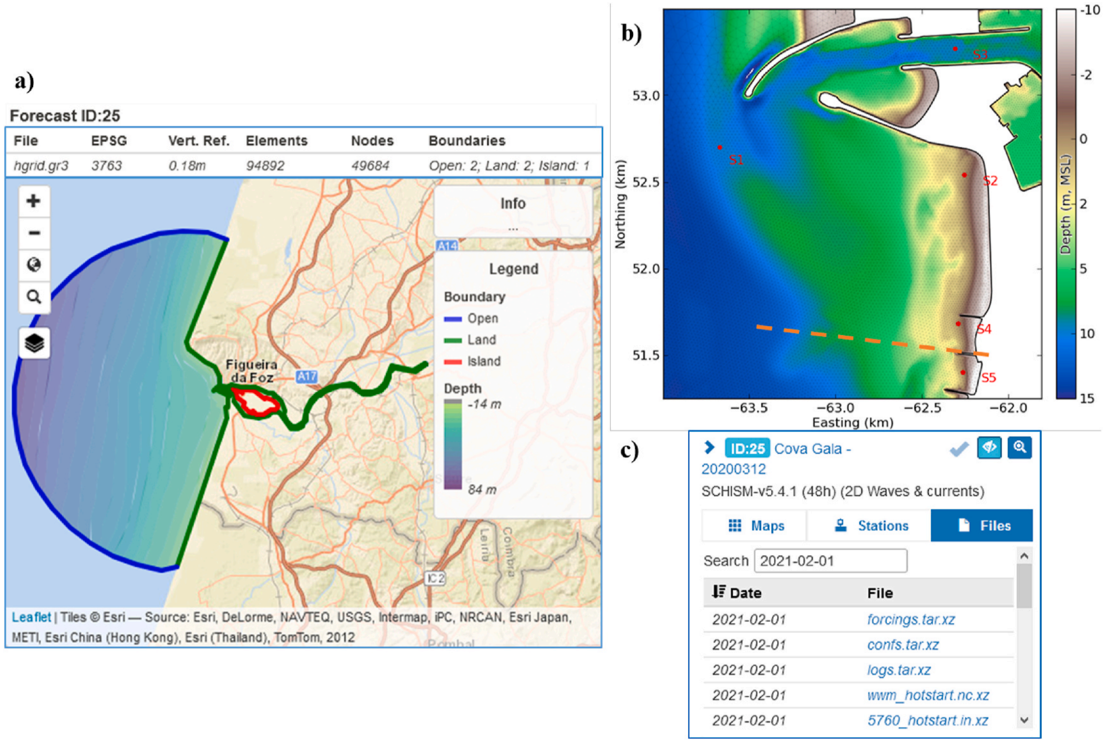

Fig. 10. Figueira da Foz Forecast system: a) computational domain as seen in OPENCoastS; b) Cova Gala Beach, south of the harbor entrance, with the location of the output stations (S1-S5) and of the bathymetric profile shown in Fig. 11a (dashed orange line); c) OPENCoastS tool to download daily files containing forcings, hotstarts and model results.

Table 3
Bias and root mean square errors (RMSE) between modeled and observed significant wave height (Hs) and water level elevation across the computational domain (after Nahon et al., 2020).

	Hs		Elevation	
	Bias (% of mean)	RMSE (% of mean)	Bias (m)	RMSE (m)
Offshore: Wave buoy	−13.4	20.4	–	–
Nearshore: Pressure transducers	−17.3 < . < 12.4	13.9 < . < 20.0	0.13 < . < 0.26	0.14 < . < 0.26
Harbor: Tidal gauge	–	–	−0.01	0.04
Upstream: Tidal gauge	–	–	−0.07	0.12

the 2019 bathymetry (Fig. 11a). In the second bathymetry, the nearshore area was changed to a state representative of summer 2018.

3.3.3. *Duplicated forecasts and hydrodynamic results*

All input files and forcings were downloaded from the OPENCoastS service web app using the Files download tool accessible within the Outputs viewer (Fig. 10c): input files from 1 February 2021 were used with circulation initial conditions created on 31 January 2021. The model was then run offline for the three bathymetric configurations.

Simulations were analyzed at five virtual output stations (Fig. 10b), although here results were outputted every 10 min compared to 1 h outputs within OPENCoastS. Stations S1-S3 were placed to evaluate the sensitivity of the harbor hydrodynamics to bathymetric changes induced by storm Epsilon. Stations S4-S5 were placed shoreward of the 2018 sediment disposal location to analyze the impact of the dredging spoils on the beach hydrodynamics.

The simulated period covered the 2nd storm modeled in the previous case study in the Bay of Biscay. Here, the offshore significant wave height peaked at 6.9 m at 15:00 on 1 February, before the high tide of a moderate 2.5 m tidal cycle. At stations S1-S3, the main differences concerned the significant wave height and the current velocities, and were largest within the access channel (S1, Fig. 12). At S1, compared to the configuration with a well-defined channel, the post-storm configuration showed a modest decrease of 5% of the significant wave height at the peak of the storm and a stronger increase of the current velocities, on the order of 20%. Differences at the beach (S2, 0 m depth MSL) are less pronounced, likely because the surfzone was saturated and the wave height was controlled by the depth-induced breaking. In the 9-m deep main harbor channel (S3), differences in velocities were negligible. In contrast, the wave height was affected by up to 25% although this concerned waves with a modest size. However, phase-averaged models such as WWM only provide an approximate representation of wave diffraction which may limit the accuracy of the wave predictions between the jetties. Also, WWM does not reproduce the wave reflection at the jetties.

Stations S4-S5 were placed along the 0 m depth contour, southward of the tidal inlet. Similarly to S2, differences in significant wave height were negligible. Differences in total water level reached 5 cm (Fig. 13). The main differences at those beach cells were observed in the intensity of the modeled current, with overall stronger currents, after the deposited sediment migrates shoreward (2019-09 configuration).

Overall, these results show that, although the bathymetric changes were significant, differences were modest in terms of modeled significant wave height and total water levels. The main differences occurred for the predicted current velocities in the access channel (S1) and over the intertidal beach in the shadow of the dredging spoils (S4 and S5). However, these results cannot be generalized since this analysis was made under specific wave and tidal conditions.

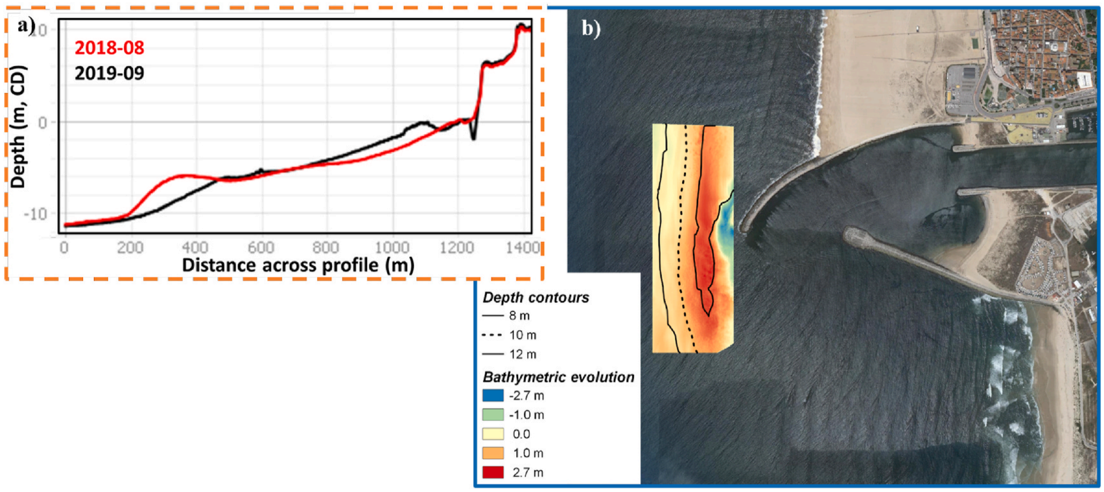

Fig. 11. Bathymetric evolution near Figueira da Foz harbor: a) bathymetric evolution of the 2018 dredging disposal (red) through to 2019 (black), along the profile plotted on Fig. 10b (dashed orange line); b) bathymetric evolution of the harbor entrance channel during storm Epsilon (October 2020) along with post-storm depth contours (positive is accretion).

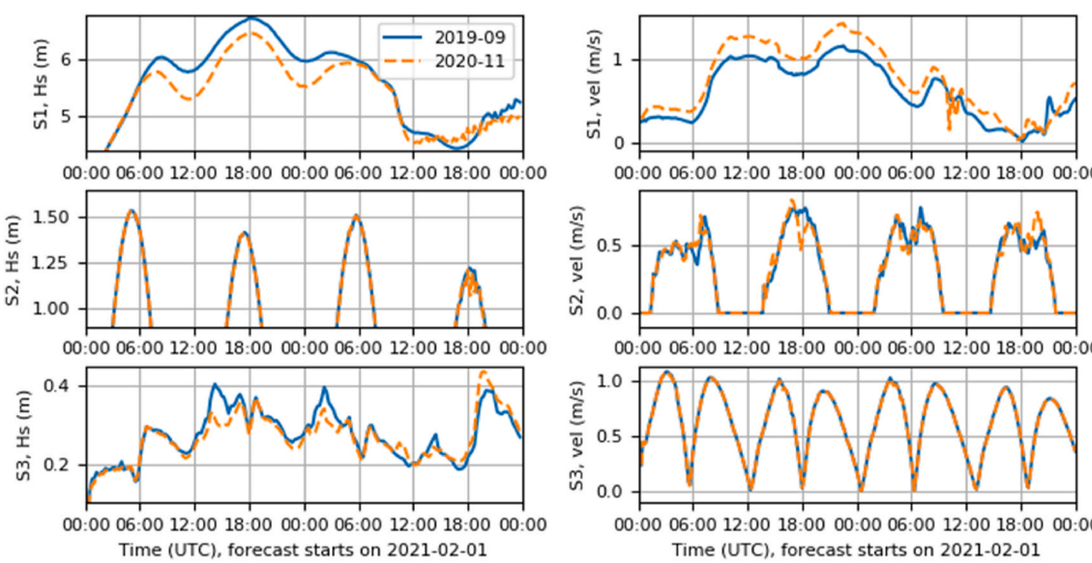

Fig. 12. Sensitivity of the significant wave height (Hs, left) and current velocities (right) to storm-driven bathymetric evolutions in late October 2020.

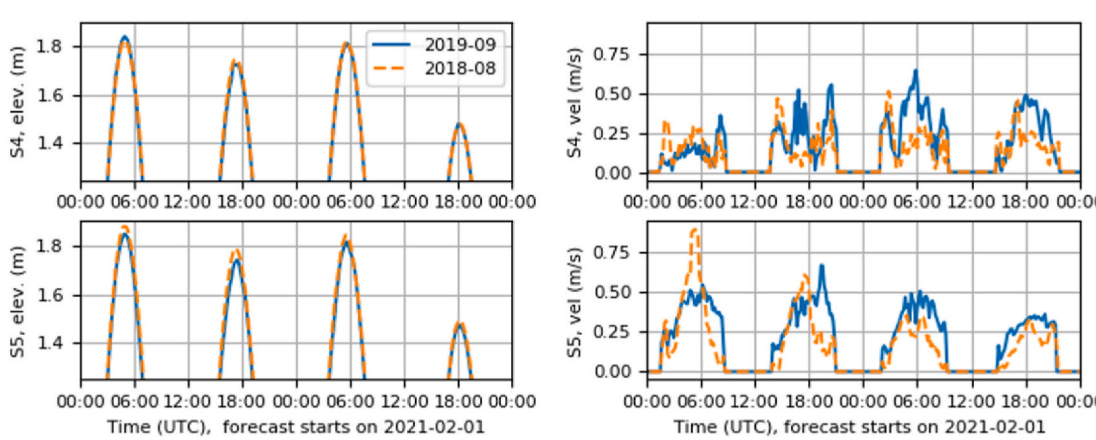

Fig. 13. Sensitivity of nearshore water levels (left) and current velocities (right) to bathymetric evolutions following the disposal of dredging material in 2018.

3.4. Tagus estuary 3D baroclinic case study

The Tagus estuary (Portugal) is one of the largest estuaries in Europe and holds a major natural reserve, which is one of the most important sanctuaries for wintering or staging birds. The estuarine margins are intensively occupied, with a population of about one million inhabitants, and support diverse uses and activities (urban, industrial/harbors, agriculture, shellfish harvesting). The estuary has a deep and narrow inlet channel and a broad and shallow inner basin. The intertidal area constitutes about 40% of the total estuarine surface (Castanheiro, 1986). Tides are the main driver of the circulation in the Tagus estuary (Fortunato et al., 2017b). Tides are semi-diurnal and range from 0.55 m to 3.86 m at the coast (Guerreiro et al., 2015). The tidal propagation within the estuary is complex and tidal amplitudes are amplified by resonance (Fortunato et al., 1997, 1999). Other drivers, such as the river flow, wind, atmospheric pressure and surface waves, also influence the circulation within the estuary. The Tagus River, with an average flow of 370 m^3/s (APA, 2012), is the main source of freshwater into the estuary. Other tributaries (the Sorraia and the Trancão rivers) also contribute to the freshwater inflow into the estuary. The estuary is usually well-mixed, but stratification can occur at high flow rates and low tidal ranges (Neves, 2010; Rodrigues and Fortunato, 2017). Residence times in the estuary result from the interaction between different factors, such as tide, river flow and wind (e.g., Oliveira and Baptista, 1997; Vaz and Dias, 2014). Several studies showed the interaction between the Tagus and the adjacent coastal area and the sediments, nutrients, plankton and fisheries dynamics in the estuary (e.g., Gameiro and Brotas, 2010; Valente and Silva, 2009). The physical drivers play an important role in these dynamics. In the Tagus estuary, residence time is the main factor influencing phytoplankton annual variability (Brotas and Gameiro, 2009), with lower concentrations occurring during wet years. Moreover, other physical factors, such as salinity can influence the biotic distribution within the estuaries (e.g. Wolf et al., 2009).

The operational model of the Tagus estuary was first implemented and validated in hindcast mode (Rodrigues and Fortunato, 2017). The model extends from the ocean to the river and the domain is discretized with a horizontal grid of about 83,000 nodes and 157000 elements, which has a typical resolution of 15–25 m (Fig. 14). The vertical domain is discretized with a hybrid grid with 39 SZ levels (30 S levels in the upper 100 m, and 9 Z levels between 100 m and the maximum depth).

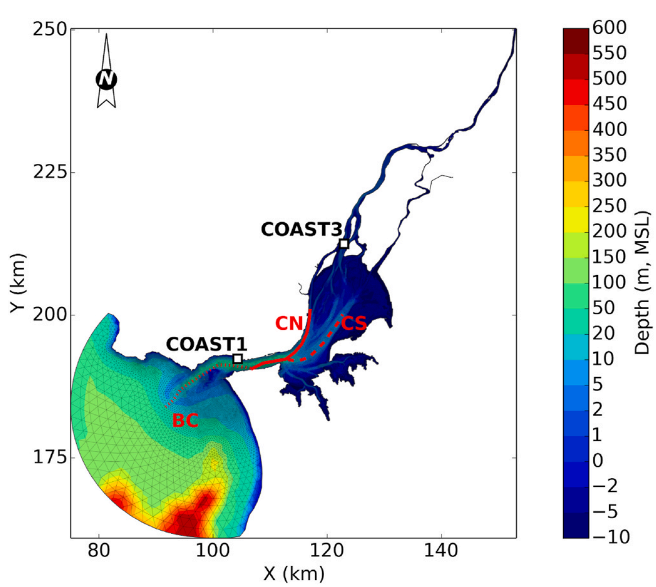

Fig. 14. Horizontal grid and location of the stations. The Almourol station, used to provide river boundary conditions, is located about 37 km upstream of the model domain.

Within OPENCoastS (Fig. 15) the model is forced by: i) sea surface heights, salinity, water temperature from the CMEMS-IBI model at the oceanic boundary; ii) extrapolation of river flows from the SNIRH Almourol station (http://snirh.apambiente.pt), zero salinity and monthly climatological values of water temperature at the riverine boundaries (Tagus and Sorraia rivers); and iii) atmospheric data at the surface from the GFS model. The time step was set to 30s.

Data from the COASTNET Portuguese monitoring network (http://geoportal.coastnet.pt/) were used to assess the operational model salinity and water temperature. The data-model comparison was performed between November 2019 and February 2020, which includes a period of high river flows susceptible to lead to stratification (Rodrigues and Fortunato, 2017), aiming to assess the operational model response for different forcing conditions.

Results show the ability of the model to represent the main variations regarding salinity and water temperature, both upstream and downstream (Fig. 16, supplementary material #2). However, the temperature is underestimated upstream, where a negative bias is observed (Fig. 16, supplementary material #2). RMSE and mean absolute error (MAE) for salinity and water temperature (Fig. 16) are typically of the same order of magnitude of previous hindcast applications (Rodrigues and Fortunato, 2017; Rodrigues et al., 2019), although slightly higher upstream. The differences observed between the data and the model forecasts may be due to the boundary conditions imposed. At the riverine boundaries, the river flow is extrapolated from the last flow measured, which may introduce phase errors in the model results (of about 1–2 days) when significant variations of the flow occur. Also, the water temperature at these boundaries is based on climatology, which constitutes a major source of uncertainty and may explain the larger differences observed in the upstream station. The atmospheric forcing may also influence the salinity and water temperature dynamics in the Tagus estuary (Rodrigues et al., 2016; Rodrigues and Fortunato, 2017) and explain some of the differences observed, since a global model with a low resolution was used.

The 3D model is able to represent the vertical dynamics of salinity and water temperature in the Tagus estuary, which is expected to become stratified for river flows higher than 1000 m3/s. The operational model represents the stratified conditions (Fig. 17 and Fig. 18) that occur during a period where river flow was about 2000 m^3/s. Results show that the riverine plume extends further into the ocean for larger river flows and leads to the stratification of the water column, with salinities near the inlet of about 20 at the surface and about 32–34 near the bottom at low tide. For a river flow of about 370 m3/s (close to the mean river flow of the Tagus river - 360 m3/s) the mixing is stronger; near the inlet salinity ranges between 30 and 34 at low tide.

Overall the forecasts proved to adequately represent the salinity and water temperature dynamics in the Tagus estuary and can provide useful information to support diverse activities in the area.

4. Discussion, conclusions and future perspectives

Over the past three years, OPENCoastS has grown from an innovative on-demand platform that addressed simple 2D barotropic forecasts to a powerful tool that solves all circulation options, used by over 400 users and applied on all continents. Most past applications are scientific ones, to understand the importance of processes at a site or to explore the influence of numerical and physical parameters or forcing sources on forecasts, among other goals. Several deployments were also built to predict site circulation, either to support field work preparation or to anticipate hazardous conditions.

The applications presented herein proved the usefulness of OPENCoastS and provided important lessons. The application to the coast of Taiwan showed that useful forecasts can be obtained using only large-scale public data. This success is very important, considering the existence of many data-poor environments worldwide without forecast systems. Also, this forecast was run with simplified physics (i.e., waves

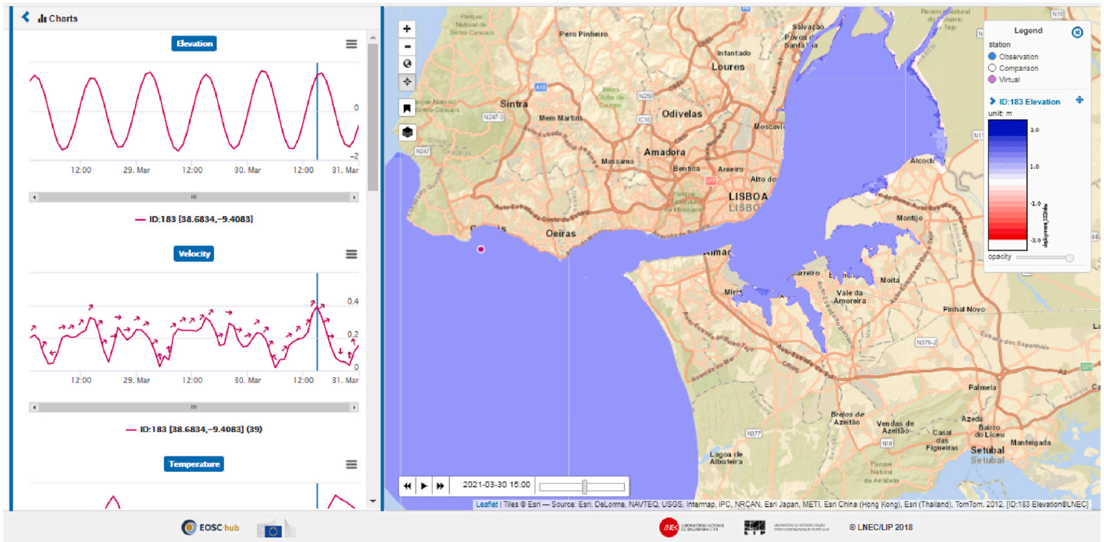

Fig. 15. Outputs viewer: Water levels and velocities at Cascais - Tagus estuary. The time series of water levels and velocities on the left were extracted at the red circle outside the mouth.

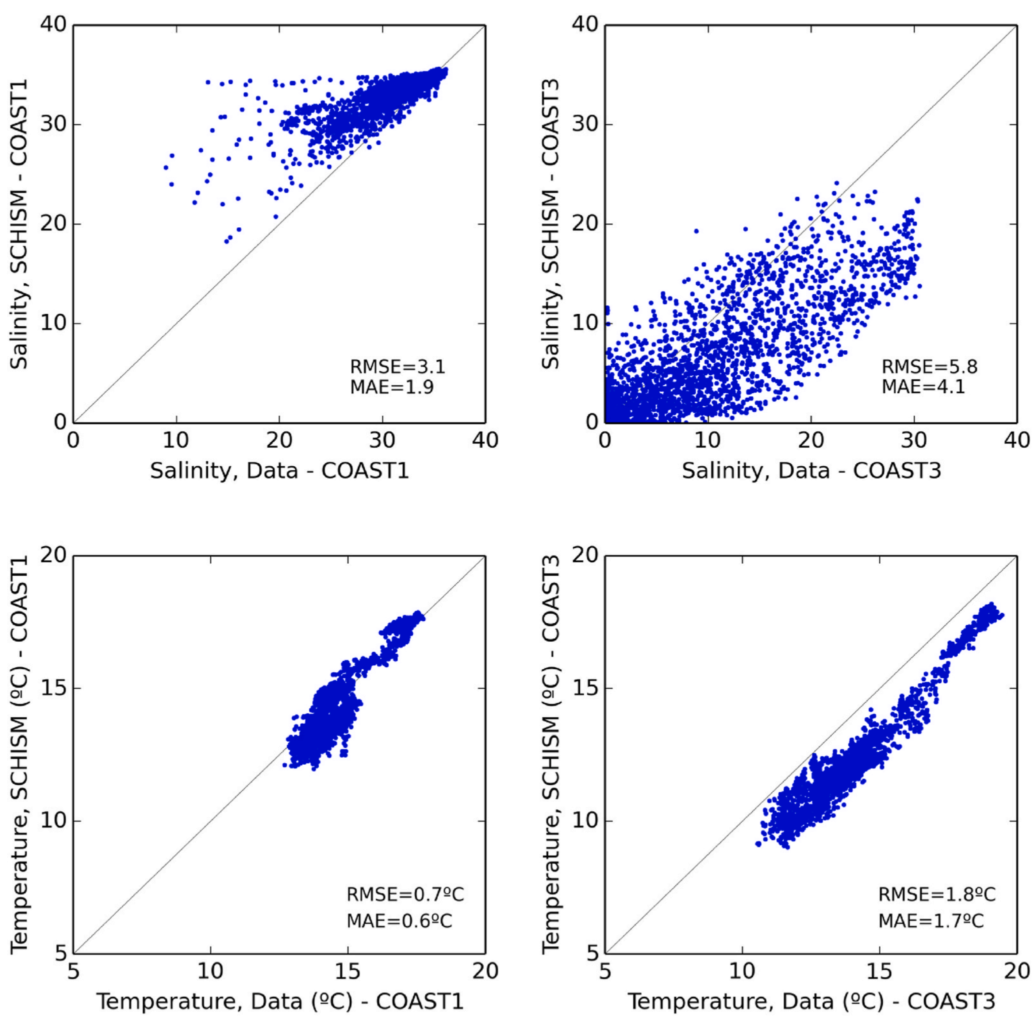

Fig. 16. Salinity and water temperature data vs SCHISM Forecasts in the Tagus estuary. Root mean square error (RMSE) and mean absolute error (MAE) for salinity and water temperature are indicated in the figures.

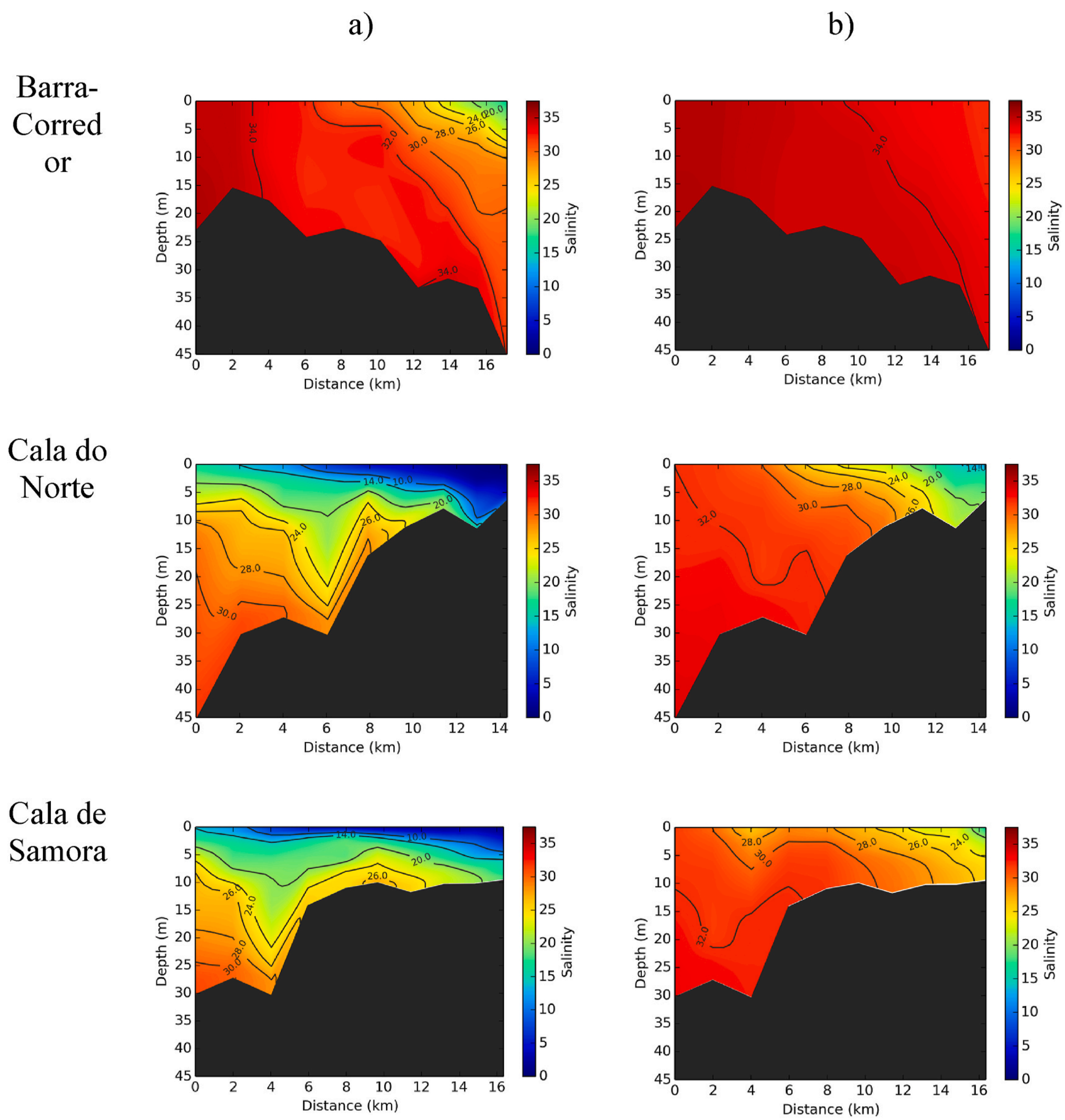

Fig. 17. Forecasted vertical profiles of salinity at low tide on a) December 23, 2019 - estimated river flow of 2000 m3/s and b) January 25, 2020 - estimated river flow of 370 m3/s (see Fig. 14 for the location of the longitudinal profiles).

were neglected). Although this simplification is still common in forecast systems (Umgiesser et al., in press), waves can play an important role in the storm surge (Lavaud et al., 2020; Liu and Huang, 2020). This role is confirmed in the Bay of Biscay application, where the inclusion of wave forces reduces the error in the storm surge by a factor of 3. To a smaller extent, the accuracy of the forecasts in shallow areas also depends on accurate and updated bathymetries. This dependence is illustrated in the Figueira da Foz harbor example. The limitations imposed by the lack of detailed data is also highlighted in the Tagus Estuary case, which suggests that absence of small-scale atmospheric predictions and river flow forecasts constitute important sources of errors. In summary, while OPENCoastS can provide useful results using only publicly available data and simplified physics, the more demanding users should include high-resolution and updated data, and include all the relevant processes. The possibility to use atmospheric predictions provided by the user is planned for future versions of OPENCoastS, similar to the current capacity to specify a source for river flow predictions.

The applications presented herein also highlight the usefulness of OPENCoastS as a tool to automate many time-consuming tasks in coastal modeling, such as the generation of input files, downloading and processing of atmospheric forecast and post-processing of model results. This automation fosters the use of models for sensitivity analyses, as illustrated by the Bay of Biscay application. Although OPENCoastS was designed to generate forecasts, the Figueira da Foz harbor application shows how it can be exploited for hindcasts, taking advantage of the automatic generation of input files.

In spite of OPENCoastS only requiring an unstructured computational grid to set up a new forecast, the availability of such grids remains a limitation for many users, in particular for those outside the academic fora. Recent developments in automatic grid generation (e.g., Roberts et al., 2019), along with the availability of global bathymetry services, have paved the way for an integration of a grid generator in the configuration assistant of OPENCoastS. The robustness of the computational engine SCHISM, even for highly skewed grids and noisy bathymetries, is paramount for the success of this task, bearing in mind the need to include the necessary grid features for a good simulation, depending on the simulation type (e.g. good representation of the channel cross-sections and dikes).

While forecasts are often much more difficult to build than simple offline applications of a specific model, thus justifying the development

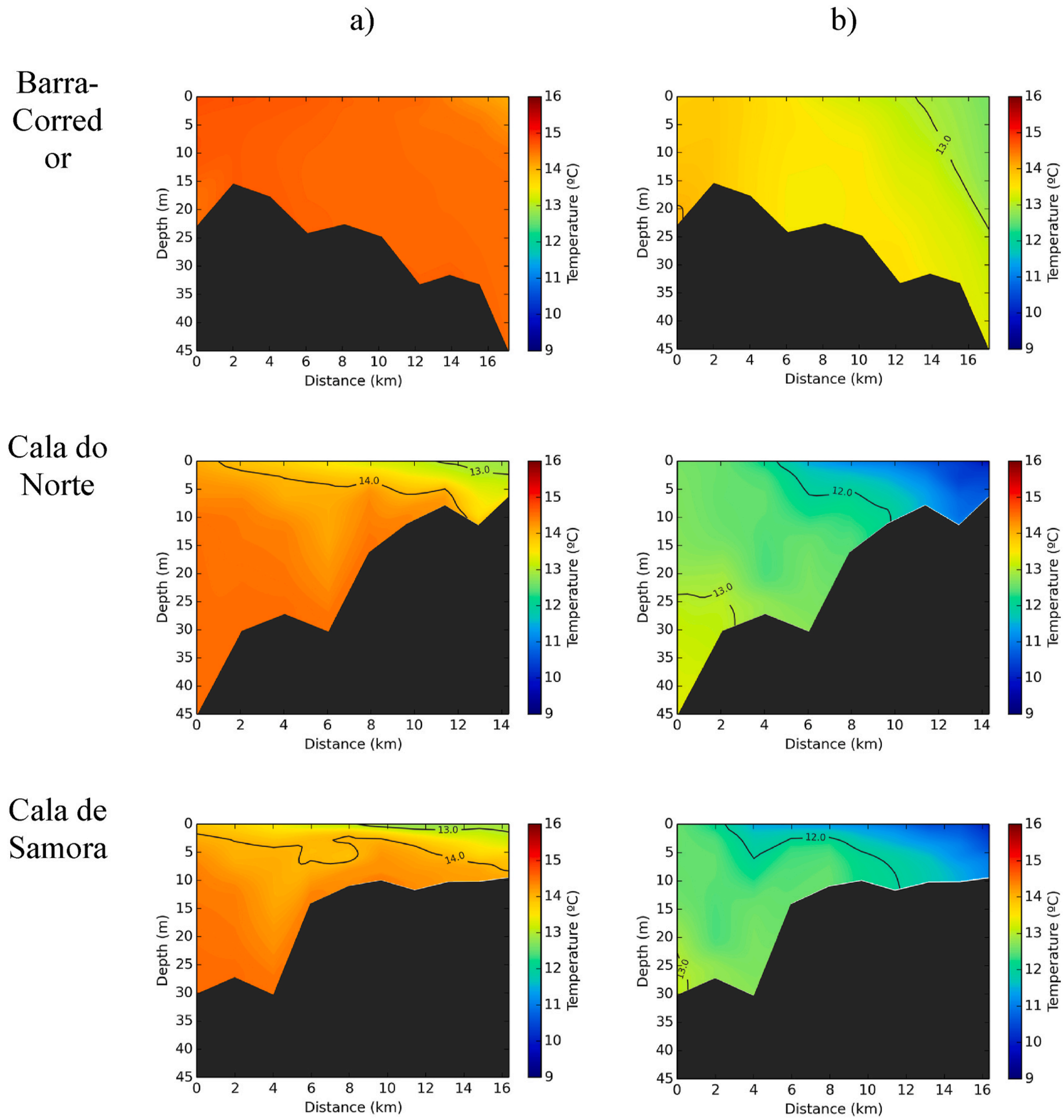

Fig. 18. Forecasted vertical profiles of water temperature on December 23, 2019 and on January 25, 2020, at low tide (see Fig. 14 for the location of the longitudinal profiles).

of sophisticated on-demand platforms such as OPENCoastS, these two tasks share a common need in high-resolution runs. These runs can be either for applications to very large domains (regional or global modeling), spatially very small events (e.g. discharge of an outfall) or multiple runs (e.g. scenarios simulation), but they all require very large computational resources. Moreover, a user-friendly platform may significantly reduce the learning curve on how to use a new model and to build on-the-fly boundary conditions from several sources. Therefore, hincast or scenario simulations are now being integrated in OPENCoastS, supported by atmospheric reanalyses and FES2014, complemented by the inverse barometer effect.

The integration of hindcast simulations in OPENCoastS raises an important issue on the evaluation of the quality of those runs. A small level of in-situ data was integrated in the platform, supported by the extensive network of EMODNET physics' water level stations and by processing Sentinel images for water/land interface detection. However, much remains to be done regarding the evaluation of salinity and temperature, waves and velocities. Better exploitation of remote sensing either from satellites (for temperature, salinity and wave comparisons) or radar networks (for surface velocities) will be considered along with a more extensive usage of EMODNET data for the same variables.

Finally, the current implementation of OPENCoastS in EOSC should also be improved to allow for better multisite scalability, elasticity, high availability and redundancy to guarantee services operation. The goals are to improve data movement between hosting infrastructure sites, using the EGI Data Transfer, and automation, scalability and elasticity using Infrastructure Manager and EGI Cloud Container Compute. Moreover, this approach will also provide an improved deployment of a distributed database solution, so that all available OPENCoastS infrastructure providers can be used transparently. This solution targets the guarantee of optimized and timely delivery of service which is fundamental for quality assurance of operational forecast systems and its high demand for immediate access to the computational resources.

Declaration of competing interest

The authors declare that they have no known competing financial interests or personal relationships that could have appeared to influence the work reported in this paper.

Acknowledgements

This work was funded by the European Commission through the H2020 projects EOSC-hub (Grant Agreement No 777536) and EOSC-Synergy (Grant Agreement No 857647), by Lisboa2020 Operational Program through the INCD project (LISBOA-01-0145-FEDER-022153) and by the Fundação para a Ciência e a Tecnologia through projects MOSAIC.pt (PTDC/CTA-AMB/28909/2017) and AQUAMON (PTDC/CCI-COM/30142/2017). This work made use of results produced with the support of the Portuguese National Grid Initiative; more information in https://wiki.ncg.ingrid.pt.

The test cases of Figueira da Foz Harbor were made thanks to bathymetric data made available by the Coastal Monitoring Programme of Continental Portugal - COSMO, co-funded within POSEUR-09-2015-25, and thanks to bathymetric data obtained within the project NAV-SAFETY, funded by the Direção-Geral de Política do Mar, in the scope of the Fundo Azul.

Appendix A. Supplementary data

Supplementary data to this article can be found online at https://doi.org/10.1016/j.envsoft.2021.105132.

References

Allan, J., Priest, G.R., Zhang, Y.J., Gabel, L., 2018. Maritime tsunami evacuation guidelines for the Pacific Northwest coast of Oregon. Nat. Hazards 94, 21–52. https://doi.org/10.1007/s11069-018-3372-2.

APA – Agência Portuguesa do Ambiente, 2012. *Plano de Gestão da Região Hidrográfica do Tejo, Relatório Técnico – Síntese*. Ministério da Agricultura, do Mar, do Ambiente e do Ordenamento do Território.

Bedri, Z., Corkery, A., O'Sullivan, J.J., Alvarez, M.X., Erichsen, A.C., Deering, L.A., Demeter, K., O'Hare, G.M.P., Meijer, W.G., Masterson, B., 2014. An integrated catchment-coastal modelling system for real-time water quality forecasts. Environ. Model. Software 61, 458–476. https://doi.org/10.1016/j.envsoft.2014.02.006.

Bertin, X., Li, K., Roland, A., Zhang, Y.J., Breilh, J.F., Chaumillon, E., 2014. A modeling-based analysis of the flooding associated with Xynthia, central Bay of Biscay. Coast. Eng. 94, 80–89. https://doi.org/10.1016/j.coastaleng.2014.08.013.

Bertin, X., Li, K., Roland, A., Bidlot, J.R., 2015. The contribution of short-waves in storm surges: two case studies in the Bay of Biscay. Continent. Shelf Res. 96, 1–15. https://doi.org/10.1016/j.csr.2015.01.005.

Breivik, O., Allen, A.A., 2008. An operational search and rescue model for the Norwegian Sea and the North Sea. J. Mar. Syst. 69 (1–2), 99–113. https://doi.org/10.1016/j.jmarsys.2007.02.010.

Brotas, V., Gameiro, C., 2009. Padrões de variabilidade sazonal e interanual de nutrientes e fitoplâncton no estuário do Tejo. Plano de Ordenamento do Estuário do Tejo, Saberes e Reflexões. Gabinete de Ordenamento do Território, Administração da Região Hidrográfica do Tejo, Ministério do Ambiente, do Ordenamento do Território e do Desenvolvimento Regional, 150-153.

Castanheiro, J.M., 1986. Distribution, transport and sedimentation of suspended matter in the Tejo Estuary. In: Estuarine Processes: an Application to the Tagus Estuary. Secretaria de Estado do Ambiente e Recursos Naturais, Lisboa, Portugal, pp. 75–90.

Chen, C., Beardsley, Robert C., Luettich Jr., Richard A., Westerink, Joannes J., Wang, Harry, Perrie, Will, Xu, Qichun, Donahue, Aaron S., Qi, Jianhua, Lin, Huichan, Zhao, Liuzhi, Kerr, Patrick C., Meng, Yanqiu, Toulany, Bash, 2013. Extratropical storm inundation testbed: intermodel comparisons in Scituate, Massachusetts. J. Geophys. Res. Oceans 118, 5054–5073. https://doi.org/10.1002/jgrc.20397.

Chiu, C., Huang, C., Wu, L., Zhang, Y., Chuang, L., Fan, Y., Yu, H.-C., 2018. Forecasting of oil-spill trajectories by using SCHISM and X-band radar. Mar. Pollut. Bull. 137, 566–581.

Codiga, D.L., 2011. Unified Tidal Analysis and Prediction Using the Utide Matlab Functions. Graduate School of Oceanography, University of Rhode Island Narragansett, RI.

Du, J., Park, K., Shen, J., Zhang, Y.J., Yu, X., Ye, F., Wang, Z., Rabalais, N.N., 2019. A hydrodynamic model for Galveston Bay and the shelf in the northern Gulf of Mexico. Ocean Sci. 15, 951–966. https://doi.org/10.5194/os-15-951-2019.

Elsner, J.B., Liu, K.-B., 2003. Examining the ENSO-typhoon hypothesis. Clim. Res. 25, 43. https://doi.org/10.3354/cr025043.

Fernandez-Montblanc, T., Vousdoukas, M.I., Ciavola, P., Voukouvalas, E., Mentaschi, L., Breyiannis, G., Feyen, L., Salamon, P., 2019. Towards robust pan-European storm surge forecasting. Ocean Model. 133, 129–144. https://doi.org/10.1016/j.ocemod.2018.12.001.

Ferrarin, C., Davolio, S., Bellafiore, D., Ghezzo, M., Maicu, F., Mc Kiver, W., Drofa, O., Umgiesser, G., Bajo, M., De Pascalis, F., Malguzzi, P., Zaggia, L., Lorenzetti, G., Manf, G., 2019. Cross-scale operational oceanography in the adriatic sea. J. Oper. Oceanogr. https://doi.org/10.1080/1755876X.2019.1576275.

Fortunato, A.B., Baptista, A.M., Luettich Jr., R.A., 1997. A three-dimensional model of tidal currents in the mouth of the Tagus Estuary. Continent. Shelf Res. 17, 1689–1714.

Fortunato, A.B., Oliveira, A., Baptista, A.M., 1999. On the effect of tidal flats on the hydrodynamics of the Tagus estuary. Oceanol. Acta 22, 31–44.

Fortunato, A.B., Bruneau, N., Azevedo, A., Araújo, M.A.V.C., Oliveira, A., 2011. Automatic improvement of unstructured grids for coastal simulations. J. Coast. Res. Special Issue 64, 1028–1032.

Fortunato, A.B., Oliveira, A., Rogeiro, J., Tavares da Costa, R., Gomes, J.L., Li, K., Jesus, G., Freire, P., Rilo, A., Mendes, A., Rodrigues, M., Azevedo, A., 2017a. Operational forecast framework applied to extreme sea levels at regional and local scales. J. Oper. Oceanogr. 10 (1), 1–15. https://doi.org/10.1080/1755876X.2016.1255471.

Fortunato, A.B., Freire, P., Bertin, X., Rodrigues, M., Ferreira, J., Liberato, M.L.R., 2017b. A numerical study of the February 15, 1941 storm in the Tagus estuary. Continent. Shelf Res. 144, 50–64. https://doi.org/10.1016/j.csr.2017.06.023.

Gameiro, C., Brotas, V., 2010. Patterns of phytoplankton variability in the Tagus estuary (Portugal). Estuar. Coast 33, 311–323. https://doi.org/10.1007/s12237-009-9194-4.

Gomes, J., Bagnaschi, E., Campos, I., David, M., Alves, L., Martins, J., Pina, J., López-García, A., Orviz, P., 2018. Enabling rootless Linux Containers in multi-user environments: the udocker tool. Comput. Phys. Commun. 232, 84–97. https://doi.org/10.1016/j.cpc.2018.05.021.

Guérin, T., Bertin, X., Dodet, G., 2016. A numerical scheme for coastal morphodynamic modelling on unstructured grids. Ocean Model. 104, 45–53. https://doi.org/10.1016/j.ocemod.2016.04.009.

Guerreiro, M., Fortunato, A.B., Freire, P., Rilo, A., Taborda, R., Freitas, M.C., Andrade, C., Silva, T., Rodrigues, M., Bertin, X., Azevedo, A., 2015. Evolution of the hydrodynamics of the Tagus estuary (Portugal) in the 21st century. Rev. Gestão Costeira Integrada 15, 65–80. https://doi.org/10.5894/rgci515.

Huang, W., Ye, F., Zhang, Y., Park, K., Du, J., Moghimi, S., Myers, E., Pe'eri, S., Calzada, J.R., Yu, H.C., Nunez, K., Liu, Z., 2021. Compounding factors for extreme flooding around galveston Bay during hurricane harvey. Ocean Model. 158, 101735.

Lavaud, L., Bertin, X., Martins, K., Arnaud, G., Bouin, M., 2020. The contribution of short-wave breaking to storm surges: the case Klaus in the Southern Bay of Biscay. Ocean Model. 156.

Li, X., Zhong, D., Zhang, Y., Wang, Y., Wang, Y., Zhang, H., 2018. Wide river or narrow river: future river training strategy for Lower Yellow River under global change. Int. J. Sediment Res. https://doi.org/10.1016/j.ijsrc.2018.04.001.

Liu, W.-C., Huang, W.-C., 2020. Investigating typhoon-induced storm surge and waves in the coast of Taiwan using an integrally-coupled tide-surge-wave model. Ocean Eng., 107571 https://doi.org/10.1016/j.oceaneng.2020.107571.

Longuet-Higgins, M.S., Stewart, R., 1964. Radiation stresses in water waves; a physical discussion, with applications. Deep Sea Res. Oceanogr. Abstr. 11/4, 529–562.

Lyard, F.H., Allain, D.J., Cancet, M., Carrère, L., Picot, N., 2020. FES2014 Global Ocean Tides Atlas: Design and Performances. Ocean Sciences. https://os.copernicus.org/preprints/os-2020-96/.

Lynett, P.J., Gately, K., Wilson, R., Montoya, L., Adams, L., Arcas, D., Aytore, B., Bai, Y., Bricker, J.D., Castro, M.J., Cheung, K., David, C., Dogan, G., Escalante, C., Gonzalez, F.I., Gonzalez-Vida, J., Grilli, S.T., Heitmann, T.W., Horrillo, J., KaÂ¢noÃÅlu, U., Kian, R., Kirby, J.T., Li, W., Macaas, J., Nicolsky, D.J., Ortega, S., Pampell-Manis, A., Park, Y., Roeber, V., Sharghivand, N., Shelby, M., Shi, F., Tehranir, B., Tolkova, E., Thio, H., Velioglu, D., Yalciner, A., Yamazaki, Y., Zaytsev, A., Zhang, Y., 2017. Inter-model analysis of tsunami-induced coastal currents. Ocean Model. 114, 14–32.

Nahon, A., Fortunato, A.B., Azevedo, A., Oliveira, F.S.B.F., Oliveira, J.N.C., Rogeiro, J., Jesus, G., Oliveira, A., Silva, P.A., Freire, P., 2020. Implementation and validation of an operational forecasting system for nearshore hydrodynamics with OPENCoastS. In: Atas das 6as Jornadas de Engenharia Hidrográfica/1as Jornadas Luso-Espanholas de Hidrografia. Instituto Hidrográfico, Lisboa, pp. 203–206.

Neves, F.S., 2010. Dynamics and Hydrology of the Tagus Estuary: Results from in Situ Observations. PhD Thesis. Universidade de Lisboa, Portugal.

Oke, Peter R., Proctor, Roger, Rosebrock, Uwe, Brinkman, Richard, Cahill, Madeleine L., Coghlan, Ian, Divakaran, Prasanth, Freeman, Justin, Pattiaratchi, Charitha, Roughan, Moninya, Sandery, Paul A., Schaeffer, Amandine, Wijeratne, Sarath, 2016. The Marine Virtual Laboratory (version 2.1): enabling efficient ocean model configuration. Geosci. Model Dev. (GMD) 9, 3297–3307. https://doi.org/10.5194/gmd-9-3297-2016, 2016.

Oliveira, A., Baptista, A., 1997. Diagnostic modeling of residence times in estuaries. Water Resour. Res. 33, 1935–1946.

Oliveira, A., Rogeiro, J., Jesus, G., Fortunato, A.B., David, L., Rodrigues, M., Costa, J., Mota, T., Gomes, J.L., Matos, R., 2015. Sub-chapter 3.13 - real-time monitoring and forecast platform to support early warning of faecal contamination in recreational waters. In: Climate Change, Water Supply and Sanitation: Risk Assessment, Management, Mitigation and Reduction. IWA Publishing, London, pp. 102–112.

Oliveira, A., Fortunato, A.B., Rogeiro, J., Teixeira, J., Azevedo, A., Lavaud, L., Bertin, X., Gomes, J., David, M., Pina, J., Rodrigues, M., Lopes, P., 2020. OPENCoastS: an open-access service for the automatic generation of coastal forecast systems. Environ. Model. Software 124. https://doi.org/10.1016/j.envsoft.2019.104585.

Orseau, S., Huybrechts, N., Tassi, P., Kaidi, S., Klein, F., 2021. NavTEL: open-source decision support tool for ship routing and underkeel clearance management in estuarine channels. J. Waterw. Port, Coast. Ocean Eng. 147, 2. https://doi.org/10.1061/(ASCE)WW.1943-5460.0000610.

Roberts, K.J., Pringle, W.J., Westerink, J.J., Contreras, M.T., Wirasaet, D., 2019. On the automatic and a priori design of unstructured mesh resolution for coastal ocean circulation models. Ocean Model. 144, 101509.

Rodrigues, M., Fortunato, A.B., 2017. Assessment of a three-dimensional baroclinic circulation model of the Tagus estuary (Portugal). AIMS Environ. Sci. 4 (6), 763–787. https://doi.org/10.3934/environsci.2017.6.763.

Rodrigues, M., Rogeiro, J., David, L., Fortunato, A.B., Oliveira, A., 2016. Análise de sensibilidade à incerteza dos forçamentos na previsão da qualidade da água em tempo real. Atas do 13° Congresso da Água. Lisboa, Portugal), 15pp.

Rodrigues, M., Fortunato, A.B., Freire, P., 2019. Saltwater intrusion in the upper Tagus estuary during droughts. Geosciences 9 (9), 400. https://doi.org/10.3390/geosciences9090400.

Roland, A., Zhang, Y.J., Wang, H.V., Meng, Y., Teng, Y.-C., Maderich, V., Brovchenko, I., Dutour-Sikiric, M., Zanke, U., 2012. A fully coupled 3D wave-current interaction model on unstructured grids. J. Geophys. Res. 117 (C11).

Stanev, E.V., Schulz-Stellenfleth, J., Staneva, J., Grayek, S., Grashorn, S., Behrens, A., Koch, W., Pein, J., 2016. Ocean forecasting for the German Bight: from regional to coastal scales. Ocean Sci. 12, 1105–1136.

Stokes, K., Poate, T., Masselink, G., King, E., Saulter, A., Ely, N., 2021. Forecasting coastal overtopping at engineered and naturally defended coastlines. Coast. Eng. 164, 103827. https://doi.org/10.1016/j.coastaleng.2020.103827.

The WAVEWATCH III R Development Group (WW3DG), 2016. User manual and system documentation of WAVEWATCH III R version 5.16. Tech. Note 329. NOAA/NWS/NCEP/MMAB, College Park, MD, USA, p. 326.

Trotta, F., Fenu, E., Pinardi, N., Bruciaferri, D., Giacomelli, L., Federico, I., Coppini, G., 2016. A structured and unstructured grid relocatable ocean platform for forecasting (SURF). Deep Sea Res. Part II Top. Stud. Oceanogr. 133, 54–75. https://doi.org/10.1016/j.dsr2.2016.05.004.

Trotta, F., Federico, I., Pinardi, N., Coppini, G., Causio, S., Jansen, E., Iovino, D., Masina, S., 2021. A relocatable ocean modeling platform for downscaling to shelf-coastal areas to support disaster risk reduction. Front. Mar. Sci. 8, 642815 https://doi.org/10.3389/fmars.2021.642815.

Turner, P., Baptista, A.M., 1993. ACE/gredit User's Manual. Software for Semi-automatic Generation of Two-Dimensional Finite Element Grids. Center for Coastal and Land-Margin Research, Oregon Graduate Institute of Science & Technology.

Umgiesser, G., Bajo, M., Ferrarin, C., Cucco, A., Lionello, P., Zanchettin, D., Papa, A., Tosoni, A., Ferla, M., Coraci, E., Morucci, S., Crosato, F., Bonometto, A., Valentini, A., Orlic, M., Haigh, I.D., Nielsen, J.W., Bertin, X., Fortunato, A.B., Gómez, B.P., Fanjul, A.A., Paradis, D., Jourdan, D., Pasquet, A., Mourre, B., Tintoré, J., Nicholls, R.J., (in press). The prediction of floods in Venice: methods, models and uncertainty, Nat. Hazards Earth Syst. Sci. DOI: 10.5194/nhess-2020-361.

Valente, A.S., Silva, J.C.B., 2009. On the observability of the fortnightly cycle of the Tagus estuary turbid plume using MODIS ocean colour images. J. Mar. Syst. 75 (1–2), 131–137.

Vaz, N., Dias, J.M., 2014. Residual currents and transport pathways in the Tagus estuary, Portugal: the role of freshwater discharge and wind. J. Coast. Res. Special Issue 70, 610–615.

Viegas, C.N., Nunes, S., Fernandes, R., Neves, R., 2009. Streams contribution on bathing water quality after rainfall events in Costa do Estoril-a tool to implement an alert system for bathing water quality. J. Coast. Res. Special Issue 56 (part 2), 1691–1695.

Wang, Z., Chai, F., Dugdale, R., Liu, Q., Xue, H., Wilkerson, F., Chao, Y., Zhang, Y., Zhang, H., 2020. The interannual variabilities of chlorophyll and nutrients in San Francisco Bay: a modeling study. Ocean Dynam. 70, 1169–1186. https://doi.org/10.1007/s10236-020-01386-0.

Werner, M., Schellekensa, J., Gijsbersa, P., van Dijka, M., van den Akkera, O., Heynert, K., 2013. The Delft-FEWS flow forecasting system. Environ. Model. Software 40, 65–77.

Wolf, B., Kiel, E., Hagge, A., Krieg, H.-J., Feld, C.K., 2009. Using the salinity preferences of benthic macroinvertebrates to classify running waters in brackish marshes in Germany. Ecol. Indicat. 9, 837–847.

Zhang, Y., Ateljevich, E., Yu, H.-C., Wu, C.-H., Yu, J.C.S., 2015. A new vertical coordinate system for a 3D unstructured-grid model. Ocean Model. 85, 16–31. https://doi.org/10.1016/j.ocemod.2014.10.003.

Zhang, Y.J., Ye, F., Stanev, E.V., Grashorn, S., 2016. Seamless cross-scale modeling with schism. Ocean Model. 102, 64–81.